

Topography of Geographic Atrophy in Age-Related Macular Degeneration

Matthias M. Mauschitz,¹ Sofia Fonseca,¹ Petrus Chang,¹ Arno P. Göbel,¹ Monika Fleckenstein,¹ Glenn J. Jaffe,² Frank G. Holz,¹ and Steffen Schmitz-Valckenberg¹ for the GAP Study Group³

PURPOSE. To determine the topographic distribution and progression of geographic atrophy (GA) in patients with AMD.

METHODS. Fundus autofluorescence images (excitation 488, emission 500–700 nm) from 413 eyes of 413 subjects (median age, 77.0 years; inter quartile range [IQR], 72.0–82.0 years) of the Geographic Atrophy Progression (GAP) study were retrospectively analyzed. Using a modified Early Treatment Diabetic Retinopathy Study grid to divide the posterior pole into nine different subfields plus periphery, the localization, size, and progression of atrophic patches were determined. Subfields, zones (center, inner and outer), and slices (nasal, temporal, inferior, superior) were compared using the Friedman test.

RESULTS. The center and inner zones were involved in almost all eyes (>95%), while atrophy was less common in the outer zone subfields (76%). Inner zone atrophy size (median 4.00 mm²) and progression rate (0.67 mm²/year) were significantly greater than in the outer zone (0.60 mm² and 0.42 mm²/year; $P < 0.001$). There was a trend toward outer zone subfield and periphery involvement with increasing total size of atrophy. In addition, the superior outer subfield was significantly more affected by atrophy as compared with the other three outer subfields of the grid ($P < 0.001$).

CONCLUSIONS. Distribution and progression of existing GA patches depended both on the eccentricity from the center and total GA size. Central macular areas appeared most susceptible for the occurrence and expansion of GA. Refined analysis of distribution and directional spread is important to understand the natural history of the disease. This information will likely be helpful to design interventional GA clinical trials

and associated anatomical outcome measures. (ClinicalTrials.gov number, NCT00599846.) (*Invest Ophthalmol Vis Sci*. 2012;53:4932–4939) DOI:10.1167/iovs.12-9711

Geographic atrophy (GA) is the atrophic late-stage manifestation of nonexudative AMD. This disease is responsible for severe visual loss in approximately 20% of all AMD patients,^{1–6} and is characterized by the development of atrophic areas that enlarge steadily over time and are associated with a corresponding absolute scotoma. The pathophysiological mechanisms underlying disease development and progression are still poorly understood.

The term “geographic atrophy” was originally introduced because it was felt that well-demarcated borders of atrophic areas would not seem to be related to specific anatomic structures.^{1–3} Subsequently, the phenomenon of “foveal sparing” was observed (i.e., the development and enlargement of atrophy outside the fovea with involvement of the foveolar tissue late in the disease course^{4–6}). In this context, Sunness and colleagues observed in a subgroup of GA patients the coalescence of atrophic areas with development of a “horseshoe” or later “ring” configuration of atrophy surrounding the fovea.^{4,5} This pattern of disease evolution corresponds with progressive visual impairment that is initially characterized by reading difficulties due to parafoveal scotomata while the central visual acuity is preserved.⁷ Finally, when the fovea becomes involved, a dramatic loss in vision occurs.

The reason for the relative slower spread of atrophy toward the foveal center remains unclear. Given the high density of cone photoreceptors in the fovea, several authors have considered a preferential vulnerability of the rod system and relative resistance of the cone system with regard to the underlying disease process.^{8–13} Others have postulated that the unique choroidal blood supply in the fovea may be protective against atrophy involvement.^{14,15} Lastly, the high density of luteal pigment (i.e., lutein and zeaxanthin) at the level of the neurosensory retina in the central macula may impact the spread of atrophy.¹⁶

Fundus autofluorescence (FAF) imaging is a noninvasive imaging method that allows for topographic mapping of lipofuscin distribution in the RPE cell monolayer in-vivo.^{17,18} Due to the absence of RPE lipofuscin, atrophic areas in eyes with GA have a severely reduced signal. The high contrast of these hypoautofluorescent areas, compared with nonatrophic retina, allows for easy and accurate determination of lesion boundaries, particularly when compared with conventional fundus photography. Using customized image analysis software, atrophic patches can be quantified and the spread of the total size of atrophy can be determined over time.^{19,20} Previously, longitudinal natural history studies have reported mean annual progression rates of atrophy between 1.3 mm²/year and 2.6 mm²/year (Holz et al. *IOVS* 2010;51:ARVO E-Abstract 94).^{21–25}

From the ¹Department of Ophthalmology, University of Bonn, Bonn, Germany; and ²Ophthalmology, Duke University Eye Center, Durham, North Carolina.

³See the Appendix for the principal investigators in the Geographic Atrophy Progression (GAP) Study Group.

Supported by Alcon Laboratories Inc., Fort Worth, Texas. The Geographic Atrophy Progression (GAP) Study was funded, designed, and conducted by the Sponsor. The data presented is an additional analysis that was conducted without extra funding by the sponsor. The manuscript was reviewed and approved by the Sponsor.

Submitted for publication February 16, 2012; revised May 2, 2012; accepted May 25, 2012.

Disclosure: **M.M. Mauschitz**, None; **S. Fonseca**, None; **P. Chang**, None; **A.P. Göbel**, Heidelberg Engineering (F); **M. Fleckenstein**, Heidelberg Engineering (F, R), Optos Ltd. (F); **G.J. Jaffe**, Heidelberg Engineering (C); **F.G. Holz**, Heidelberg Engineering (F, C, R), Carl Zeiss Meditec AG (C), Optos Ltd. (F); **Steffen Schmitz-Valckenberg**, Heidelberg Engineering (F, C, R), Carl Zeiss Meditec AG (F), Optos Ltd (F), Topcon UK (F)

Corresponding author: Steffen Schmitz-Valckenberg, Department of Ophthalmology, University of Bonn, Ernst-Abbe-Str. 2, 53127 Bonn, Germany; steffen.schmitz-valckenberg@ukb.uni-bonn.de.

It would be useful to understand the distribution and progression patterns of GA to gain insight into disease pathogenesis, and to better design GA interventional trials and study endpoints. However, to date, there is minimal information regarding topographic spread characteristics of atrophy other than the foveal sparing phenomenon described above. Likewise, neither quantitative data on the topographic distribution nor regional/directional enlargement of atrophic areas have been reported. The aim of this study was to systematically analyze the topographic distribution of atrophic areas and their progression over time in a large natural history study in subjects with GA using FAF imaging.

METHODS

Population

Subjects were recruited from the natural history of Geographic Atrophy Progression (GAP) Study. This prospective, multicenter, noninterventional, observational study with no masking or randomization was originally designed to identify risk factors and to quantify atrophic lesion growth in patients with GA secondary to AMD. Clinical centers in the United States, Europe, Israel, and Australia participated in this endeavor. The study followed the tenets of the Declaration of Helsinki and was approved by the local ethics committees. Informed consent was obtained from each subject after explanation of the nature and possible consequences of the study. Scheduled study visits were at baseline and every 6 months for up to 18 months. The primary and secondary study objectives are not the aim of the current publication and will be reported elsewhere.

For inclusion, subjects had to be 50 years of age with a well-demarcated area of GA secondary to AMD in the study eye. The total GA lesion size had to be ≤ 17.5 mm² (approximately 7 disc areas [DA]) with one single lesion of at least 1.25 mm² (0.5 DA). Best-corrected visual acuity in the study eye had to be ≥ 35 letters (20/200 Snellen equivalent or 1.0 LogMAR). In the fellow eye, drusen ≥ 63 μ m or GA had to be present. Patients were not eligible if any signs of hemorrhage or choroidal neovascularizations were observed in either eye. At the baseline visit, all subjects underwent a complete ophthalmic examination including dilated fundus exam; retinal images were collected using confocal scanning laser ophthalmoscopy (cSLO) imaging and fundus camera photography. Each participating clinical center investigator determined eligibility. Imaging data were sent to a central reading center for analysis.

Imaging Protocol

Retinal imaging and data submission were performed according to standardized Duke Reading Center and GRADE Reading Center operating procedures. These procedures included certification of each photographer prior to the initiation of the study at his/her clinical site. All subjects underwent cSLO retinal imaging (Heidelberg Retina Angiograph, HRA classic, HRA2 or Spectralis; Heidelberg Engineering, Heidelberg, Germany) that included acquisition of near-infrared reflectance (IR 820 nm), blue reflectance (BR, 488 nm [HRA2 and Spectralis] or 512 nm [HRA classic]) and FAF (exc 488 nm, em 500–700 nm). Images were recorded with a minimum resolution of 512×512 pixels. The field of view was set at $30^\circ \times 30^\circ$ and centered on the macula. For the FAF modality, two additional fields were obtained, one temporal to the macula and the other nasal to the macula centered on the temporal aspect of the optic disc. Retinal imaging data were uploaded by each clinical site through a secure website to an electronic database. Images were then assigned to readers who analyzed the images according to predefined grading parameters, including FAF pattern classification and atrophy configuration (unifocal/multifocal).^{21,26} The total GA size was assessed by semiautomated customized image analysis software according to standard operating procedures as previously

described.^{19,27} According to these procedures, follow-up images were aligned to each corresponding baseline image and the individual baseline image scale factor was used for all images of the same eye to determine the total atrophy size in mm² at each visit. This factor is based on a Gullstrand eye, assuming standard corneal radii and taking into account the individual spherical refraction as adjusted by the operator during image acquisition.²⁸ This represents an estimation of absolute area size values. For each visit, a grading report was generated, signed, and archived. Additionally, processed images with atrophic lesion boundaries automatically outlined in white were electronically saved.

Image Grading

For the current analysis, the processed images of the GA quantification procedure were used with lesion boundaries outlined in white color. A modified Early Treatment Diabetic Retinopathy Study (ETDRS) grid was placed on the foveal center with a horizontal line at the outer edge crossing through the optic disc (Fig. 1). To identify the foveal center, the distribution of macular pigment (if present in case of foveal sparing) and the shape of the retinal vessels (assuming the foveal center to be approximately 15° temporal and approximately 0.5° inferior to the center of the optic nerve head) were used as landmarks.²⁹ Using the grid, the posterior pole was divided into nine different subfields and periphery. The diameters of the grid were set to 1200 μ m, 3600 μ m, and 7200 μ m. The layer function of a graphics editing program (Adobe Photoshop CS4; Adobe Systems Inc, San Jose, CA) was applied to all images in a series to ensure that the grid was placed at exactly the same position for all visits of each study eye.

The grading was performed by two independent readers (MMM and SF) following senior review (SSV). Reader tasks included placement of the ETDRS grids on the foveal center, documentation of the GA presence/absence in every subfield, and—in case of GA presence—the quantification of total atrophy area size in every individual subfield using the previously described customized, semiautomated image analysis software.¹⁹ Measurement results were automatically exported to a commercial spreadsheet application (Microsoft Excel; Microsoft Inc, Redmond, WA) for further analysis. The placement of the grid and the quantification of subfield atrophy was reviewed by the senior grader. In addition, the sum of all subfields of every visit was compared with the originally reported total size of atrophy of the GAP Study for plausibility testing.

Statistical Analysis

Data were compiled in a spreadsheet application and analyzed using statistical analysis software (SPSS 18; IBM SPSS Statistics, Chicago, IL). Statistical analysis included frequency and descriptive statistics. The following definitions were used: The central subfield was defined as the central zone, the four subfields between the center and middle circles as the middle zone, and the four subfields between the middle and outer circles as the outer zone, respectively. Any atrophy beyond the ETDRS grid was considered atrophy in the periphery. Furthermore, the data of each of the two superior, inferior, nasal, and temporal subfields were summarized in four “slices.” The atrophy size (area in mm²) at the last available visit was subtracted from the baseline visit atrophy size (assuming a linear growth rate) to calculate the atrophy progression rate. If no atrophy was present at the last visit in a certain subfield, zone or slice, the progression rate was set to zero.

The size and progression rate of atrophy in different subfields, zones, and slices was compared with each other using the Friedman test. Statistical significance was set at $P < 0.05$.

RESULTS

Patients Characteristics

A total of 413 eyes of 413 subjects with GA and a median age of 77 years (interquartile range [IQR] 72–82 years) were

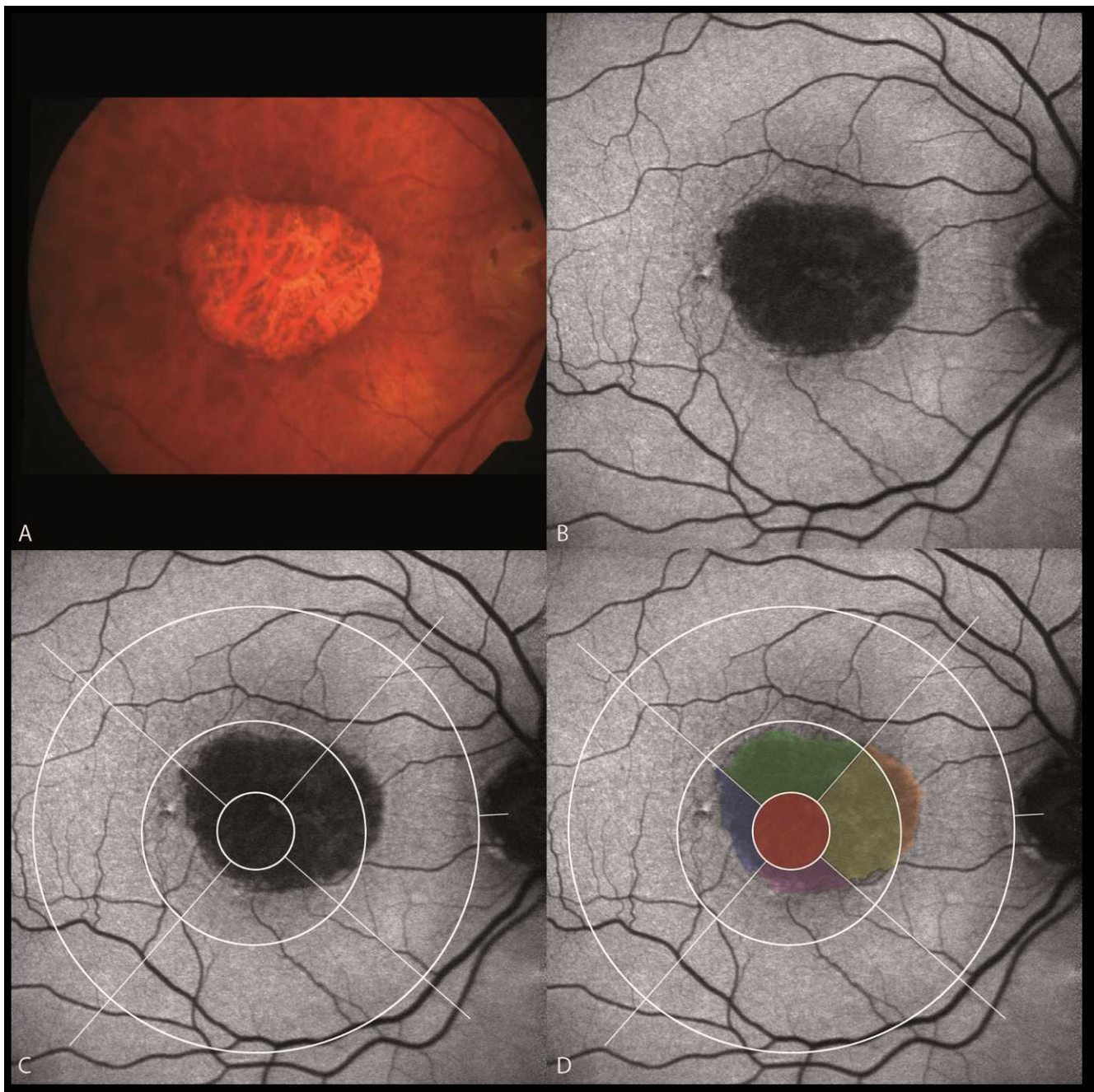


FIGURE 1. Illustration of the analysis of the atrophy topographic extent. (A) Color fundus photography. (B) Corresponding native FAF image. (C) A modified ETDRS grid was placed on the foveal center with a horizontal line at the outer edge of the grid crossing through the optic disc. (D) The atrophy involvement of the affected subfields is shown in different colors.

included in the analysis. There were 169 (41%) men and 244 (59%) women. The median total GA size for all eyes at baseline was 6.13 mm² (IQR 2.95, 10.1). Of these 413 subjects at baseline, longitudinal data at month 6 was available for 316, at month 12 for 161, and at month 18 for 41 subjects. The limited follow-up data is mainly due to early termination of subjects in the GAP study who were then enrolled in the Geography Atrophy Treatment Evaluation (GATE) study (ClinicalTrials.gov number, NCT00890097). Using the difference between the last available visit and the

baseline visit for each subject, the median progression rate was 1.49 mm²/year (range, 0.06–7.33).

Topographic Presence of Atrophy

The distribution of the presence of any atrophy for each subfield, zone, and slice is illustrated in Figure 2 (*upper row*). The center and inner zones were involved in almost all subjects (>95%), while atrophy was less commonly observed in the outer zone. Retinal areas beyond the ETDRS grid were affected

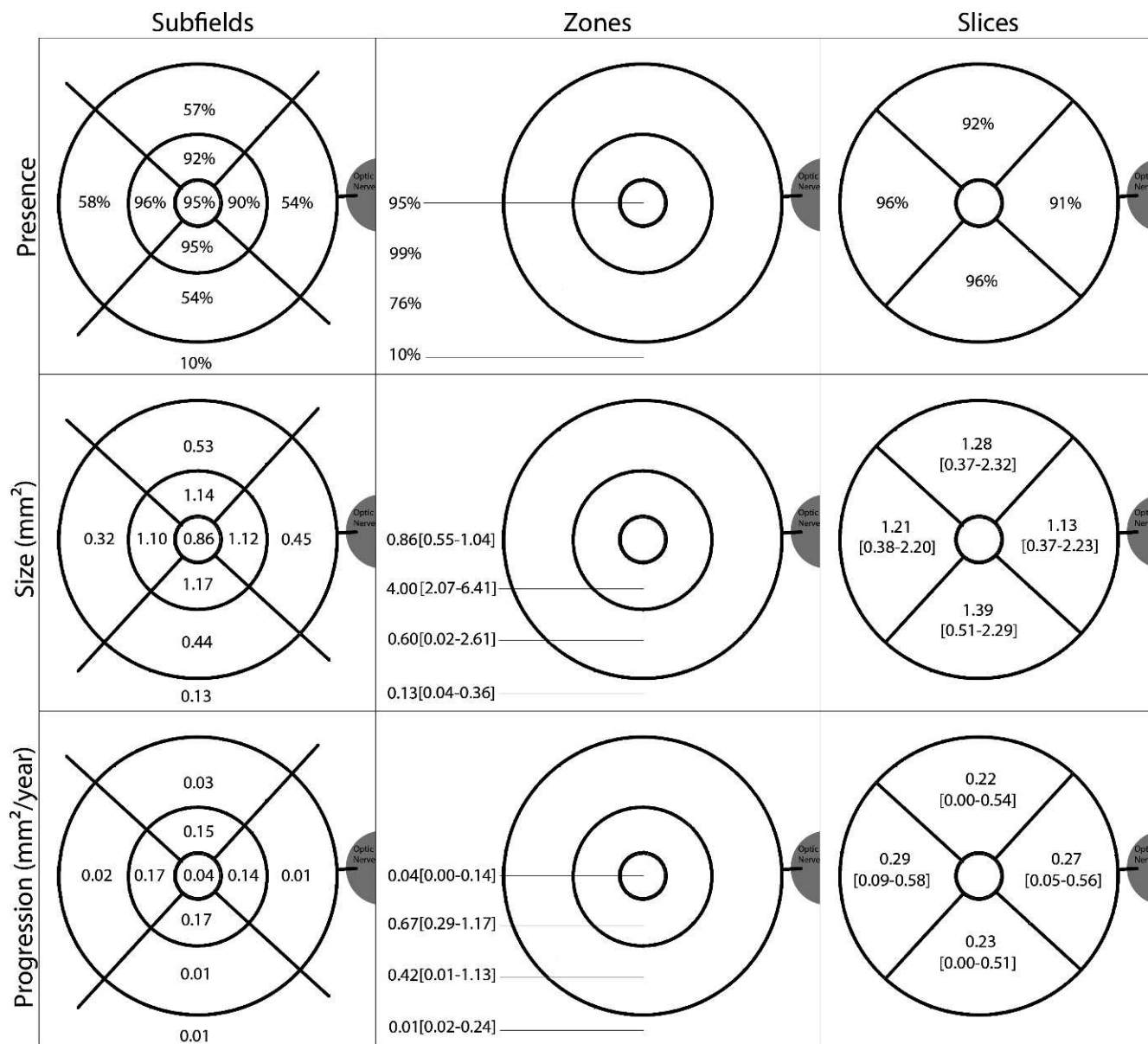


FIGURE 2. Overview of the presence, extent, and progression of atrophy. The presence (upper row), median size (middle row), and progression rates (bottom row) of atrophy are shown for each subfield (first column). Furthermore, the involvement for the center zone (center subfield), the inner zone (four subfields between center and middle circle) and outer zone (four outer subfields) and beyond the grid (“periphery”) is illustrated (second column). Finally, the data for each of the two superior, inferior, nasal, and temporal subfields of the inner and outer zones are summarized in so-called “slices” (third column). Quantitative data for size and progression rate are shown with median and IQR.

in only 10%. There was no obvious atrophy predilection for superior, inferior, nasal, or temporal regions.

Topographic Quantification of Atrophy

The topographic distribution for atrophy quantification is illustrated for each subfield, zone, and slice in Figure 2 (middle row). The median atrophy size within the center zone was 0.86 mm². That corresponded, given the mathematically possible size of 1.13 mm², to 75% of maximum area involvement. The inner zone was with a median size of 4.00 mm² (2.07–6.41) significantly more affected as compared with the outer zone with 0.60 mm² (0.02–2.61; $P = 0.001$; Fig. 2, middle row, second column; Table 1), even though the maximum possible size for the former was approximately one-third of the latter.

Within the subfields of the inner zone, similar involvement with respect to size of atrophy was observed ($P = 0.051$). By contrast, the topographic distribution of atrophy within the four subfields of the outer zone was significantly different ($P < 0.001$); the atrophy size was largest in the superior outer subfield as compared with the other three subfields of the outer zone (Fig. 3). There were no statistically significant atrophy size differences among the four slices (Fig. 2, middle row, third column).

Topographic Atrophy Progression over Time

The progression of atrophy for each subfield, each zone, and each slice is illustrated in Figure 2 (lower row). When each subfield is considered separately, only minor atrophy spread

TABLE 1. Atrophy Size at Baseline (in mm²)

	All Eyes	None + Focal	Diffuse + Banded	Unifocal	Multifocal
Inner zone	<i>P</i> = 0.051	<i>P</i> = 0.40	<i>P</i> = 0.02	<i>P</i> = 0.005	<i>P</i> = 0.06
Nasal	1.12 (0.50; 1.77)	0.72 (0.29; 1.40)	1.16 (0.62; 1.85)	1.12 (0.45; 1.79)	1.13 (0.57; 1.78)
Temporal	1.10 (0.43; 1.80)	0.65 (0.28; 1.64)	1.15 (0.48; 1.79)	1.17 (0.39; 1.94)	1.10 (0.46; 1.77)
Superior	1.14 (0.47; 1.80)	0.74 (0.28; 1.46)	1.25 (0.55; 1.88)	0.84 (0.38; 1.77)	1.21 (0.51; 1.82)
Inferior	1.17 (0.53; 1.81)	0.73 (0.34; 1.62)	1.30 (0.69; 1.85)	1.04 (0.51; 1.91)	1.21 (0.55; 1.78)
Outer zone	<i>P</i> < 0.001	<i>P</i> = 0.08	<i>P</i> = 0.003	<i>P</i> = 0.32	<i>P</i> = 0.003
Nasal	0.45 (0.15; 1.10)	0.43 (0.14; 1.07)	0.49 (0.16; 1.13)	0.35 (0.14; 1.13)	0.50 (0.17; 1.19)
Temporal	0.32 (0.10; 1.04)	0.29 (0.09; 1.33)	0.32 (0.10; 1.00)	0.38 (0.10; 1.13)	0.32 (0.11; 1.05)
Superior	0.53 (0.14; 1.31)	0.26 (0.02; 0.83)	0.55 (0.16; 1.29)	0.44 (0.07; 1.44)	0.54 (0.15; 1.21)
Inferior	0.44 (0.14; 1.10)	0.30 (0.10; 1.20)	0.35 (0.10; 0.92)	0.26 (0.08; 1.36)	0.39 (0.10; 0.95)
Slices	<i>P</i> = 0.13	<i>P</i> = 0.34	<i>P</i> = 0.04	<i>P</i> = 0.006	<i>P</i> = 0.06
Nasal	1.13 (0.37; 2.23)	0.66 (0.24; 1.47)	1.26 (0.45; 2.36)	0.89 (0.21; 2.04)	1.24 (0.45; 2.39)
Temporal	1.21 (0.38; 2.20)	0.62 (0.24; 1.91)	1.28 (0.43; 2.23)	1.19 (0.31; 2.18)	1.26 (0.43; 2.33)
Superior	1.28 (0.37; 2.32)	0.62 (0.13; 1.48)	1.49 (0.49; 2.57)	0.74 (0.18; 1.70)	1.49 (0.48; 2.51)
Inferior	1.39 (0.51; 2.29)	0.70 (0.21; 1.72)	1.45 (0.61; 2.28)	0.95 (0.35; 1.97)	1.38 (0.54; 2.26)
Inner vs. outer	<i>P</i> < 0.001				
Inner	4.00 (2.07; 6.41)	2.42 (1.42; 5.14)	4.45 (2.24; 6.75)	3.41 (1.75; 6.38)	4.25 (2.18; 6.69)
Outer	0.60 (0.02; 2.61)	0.04 (0; 0.86)	1.00 (0.13; 3.32)	0.06 (0; 1.27)	1.00 (0.17; 3.36)

Results of the statistical analysis for quantitative atrophy involvement at baseline. The four sectors of the inner zone, outer zone, and the four slices were compared with each other. In addition, the values of the four sectors of the inner zone were grouped and compared with the grouped values of the four sectors of the outer zone. This analysis was performed for all eyes and within the eyes with the none + focal and diffuse + banded FAF pattern. Finally, the size of atrophy was investigated within unifocal and multifocal GA eyes. Below the *P* values (Friedman test), the mean, and quartiles are listed. Statistical significant *P* values are written in bold script.

was observed in the center zone, outer zone and beyond the grid, while the inner zone had rapid atrophy enlargement. Regarding the individual subfields of both the inner and the outer zones (i.e., subfields with the same size), no significant difference in atrophy progression was identified (inner zone, *P* = 0.125; outer zone, *P* = 0.056; Table 2), suggesting no predilection of GA spread over time in a certain direction (nasal, temporal, inferior, or superior) from the center. Although the area of the inner zone, 9.05 mm², was smaller as compared with the outer zone, 30.54 mm², the rate of progression was significantly larger for the former (median, 0.67 mm²/year) as compared with the latter (median, 0.42 mm²/year; *P* < 0.001).

Topography and Total Size of Atrophy

The predominance of atrophy involvement in the center and inner zone compared with the outer zone and periphery was confirmed when the size of each subfield was plotted against the total atrophy size (Figs. 4A, 4B). Regarding the center zone, marked atrophy involvement was already observed in eyes with a total size of atrophy <2.5 mm² (median, 0.57 mm²), while eyes with a total size of atrophy >17.5 mm² could still have spared central zone areas (median, 0.83 mm²). The extent of atrophy, up to a total size of 17.5 mm², was largest in the inner zone. In eyes with a total size >17.5 mm², the subfields of the inner zone were almost completely involved by atrophy (median, 8.86 mm²; area size of the inner zone 9.05, mm²). According to the larger size of the outer subfields, the atrophy involvement in the outer zone then exceeded the atrophy extent of the inner zone. The outer zone was less affected than the center zone in eyes with a total size <7.5 mm². With increasing total atrophy size, the relative proportion of outer zone involvement steadily increased. In the periphery, atrophy involvement was even less compared with the center zone in eyes with a total size >17.5 mm².

FAF Patterns and Number of Atrophic Areas

At baseline, of the 413 included eyes, 291 (70%) had either a “banded” or “diffuse” FAF pattern and 68 (16%) had either the

“focal” or “none” pattern.²⁶ Unifocal GA was observed in 107 eyes (26%), while 306 (74%) had more than one atrophic spot (multifocal GA). Statistical analysis showed the predominance of the inner zone compared with the outer zone in both FAF pattern subgroups (none + focal and diffuse + banded) and for both unifocal and multifocal GA subgroups with respect to atrophy size at baseline and atrophy progression (Tables 1, 2). Eyes in the groups of unifocal GA and none + focal FAF pattern did not show any further significant differences in atrophy distribution. Within the four subfields of the outer zone, there was a statistically significant difference in the extent of atrophy for the diffuse + banded and multifocal GA subgroups. Similar

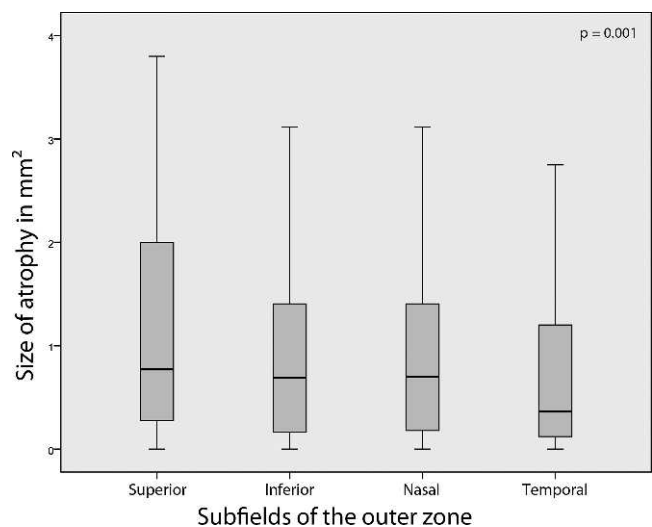


FIGURE 3. Size of atrophy in each of the different outer zone subfields as illustrated by box-and-whisker plot. The bottom top and top of each box plot illustrate the 25th and 75th percentile, respectively. The band near the middle of the box is the 50th percentile (median). The ends of the whiskers represent the minimum and maximum of all the data.

TABLE 2. Progression per Year

	All Eyes	None + Focal	Diffuse + Banded	Unifocal	Multifocal
Inner zone	$P = 0.125$	$P = 0.136$	$P = 0.261$	$P = 0.327$	$P = 0.371$
Nasal	0.14 (0.01; 0.33)	0.07 (0; 0.24)	0.17 (0.03; 0.36)	0.10 (0.01; 0.24)	0.16 (0.01; 0.35)
Temporal	0.17 (0.03; 0.34)	0.12 (0.03; 0.26)	0.18 (0.03; 0.36)	0.09 (0.01; 0.25)	0.18 (0.05; 0.35)
Superior	0.15 (0.03; 0.31)	0.11 (0; 0.26)	0.16 (0.04; 0.33)	0.09 (0; 0.20)	0.17 (0.05; 0.33)
Inferior	0.17 (0.03; 0.34)	0.14 (0.01; 0.29)	0.18 (0.04; 0.35)	0.09 (0.02; 0.27)	0.18 (0.04; 0.35)
Outer zone	$P = 0.056$	$P = 0.583$	$P = 0.009$	$P = 0.162$	$P = 0.032$
Nasal	0.01 (0; 0.29)	<0.01 (0; 0.15)	0.05 (0; 0.32)	<0.01 (0; 0.04)	0.04 (0; 0.32)
Temporal	0.02 (0; 0.29)	<0.01 (0; 0.13)	0.07 (0; 0.33)	<0.01 (0; 0.04)	0.06 (0; 0.33)
Superior	0.03 (0; 0.37)	<0.01 (0; 0.11)	0.13 (0; 0.45)	<0.01 (0; 0.01)	0.12 (0; 0.41)
Inferior	0.01 (0; 0.26)	<0.01 (0; 0.09)	0.09 (0; 0.30)	<0.01 (0; 0.01)	0.08 (0; 0.29)
Slices	$P = 0.224$	$P = 0.111$	$P = 0.007$	$P = 0.760$	$P = 0.002$
Nasal	0.27 (0; 0.50)	0.15 (0.01; 0.37)	0.35 (0.12; 0.61)	0.16 (0.01; 0.34)	0.31 (0.09; 0.63)
Temporal	0.29 (0; 0.47)	0.17 (0.05; 0.37)	0.35 (0.14; 0.69)	0.17 (0.04; 0.34)	0.32 (0.12; 0.66)
Superior	0.22 (0; 0.54)	0.19 (0; 0.38)	0.40 (0.15; 0.70)	0.13 (0; 0.29)	0.38 (0.13; 0.71)
Inferior	0.23 (0; 0.51)	0.21 (0.05; 0.46)	0.36 (0.14; 0.59)	0.16 (0.02; 0.32)	0.36 (0.14; 0.64)
Inner vs. outer	$P < 0.001$	$P < 0.001$	$P = 0.034$	$P < 0.001$	$P = 0.003$
Inner	0.67 (0.06; 1.05)	0.51 (0.25; 0.95)	0.78 (0.36; 1.32)	0.37 (0.17; 0.90)	0.76 (0.32; 1.26)
Outer	0.42 (0; 0.93)	0.15 (0; 0.80)	0.54 (0.11; 1.19)	<0.01 (0; 0.20)	0.55 (0.10; 1.28)

Results of the statistical analysis for rates of atrophy progression over time. For details, see legend for Table 1.

to the results of all eyes together, without regard to pattern subtype, the analysis showed that the largest size of atrophy was predominantly found in the superior outer subfield. In the two subgroups of diffuse + banded and multifocal GA, atrophy progressed faster in the superior compared with the other three subfields ($P = 0.009$ and $P = 0.032$). This phenomenon was not only observed for the subfields of the outer zone, but also for the superior slice ($P = 0.007$ and $P = 0.002$).

DISCUSSION

This study demonstrates that the inner zone of the ETDRS grid is the epicenter of GA location and progression in eyes with advanced non-neovascular AMD. The less frequent occurrence of atrophic areas in the outer zone and beyond the applied ETDRS grid would suggest that these retinal areas are less vulnerable and may, therefore, not represent the primary site of disease evolution.

The quantitative analysis herein confirms the previously noted descriptive observations of the foveal sparing phenomenon in the context of GA.⁴⁻⁶ Particularly, the preservation of the residual center zone area, even in eyes with very large total atrophy size, is in accordance with complete foveolar involvement only late in the disease course. As previously speculated, this phenomenon may possibly relate to the high density of cones in the central retina, possible protective effects of macular pigment and/or the unique choroidal blood supply of the fovea.⁸⁻¹⁶ In this regard, we hypothesize that the slight, but still statistically significantly larger atrophy involvement of the superior outer subfield compared with the other outer zone subfields may be caused by decreased perfusion due to gravity of retinal areas above the fovea compared with areas below the fovea. Interestingly, reticular drusen as a typical disease comanifestation of GA patients are also more prevalent in the superior outer part of the retina.^{29,30}

The quantitative data obtained in this study has important functional implications. In the presence of a horseshoe or ring-like GA configuration, the assessment of central visual acuity poorly reflects the actual visual impairment of the patient when daily visual tasks such as reading speed are considered.⁷ Furthermore, the ability of the patient to spot a single letter on the test chart may be misinterpreted as good visual function in

daily life. Additionally, the more extensive atrophy that affects the superior outer subfield, resulting in lower visual field deficits, would cause difficulty with daily living activities such as walking and climbing stairs.

Previous studies have investigated visual function in relation to the size and location of scotomata, in eyes with scotomata unrelated to AMD-associated GA.^{31,32} Visual acuity was determined as a function of foveal eccentricity; visual acuity dropped to 5° (20/200) eccentric to the foveal center. Furthermore, reading was severely compromised in patients with manifest scotomata in the central 5° field. This scenario would roughly correlate with involvement of the center and inner zone of the ETDRS grid applied in the current study. Subjects with a total GA size >17.5 mm² showed overall nearly complete atrophy involvement in those areas. Assuming that absolute scotoma are spatially confined to areas of atrophy, it would be likely that such affected individuals have already lost major macular function. Furthermore, we would expect that any treatment to stop or reduce disease progression would be less likely to benefit the daily visual function for individuals with a total GA size >17.5 mm². Accordingly, in interventional GA treatment trials, we would recommend excluding subjects with a GA area >17.5 mm².

The strengths of the study include the use of data from a large-scale multicenter natural history study, certification of study site photographers to obtain high-quality images, prospective data collection according to standardized image acquisition, and submission procedures and evaluation of images by experienced readers at a central reading center. However, limitations need to be considered. The follow-up period was limited, which was in part due to the rollover into an interventional trial (GATE study). Furthermore, the exact positioning of the ETDRS grid represented a challenge, particularly in patients with extensive foveal disease involvement. Nevertheless, it is unlikely that the major study findings would be affected by an assumed minimal misplacement of the ETDRS grid in a subset of subjects. Current knowledge suggests that GA is a heterogeneous disease with several phenotypes.²⁶ Due to the inclusion and exclusion criteria of the GAP study, a selection bias in the analysis cannot be ruled out.

Notably, the ETDRS grid-defined macular areas that include center, inner, and outer zones do not correspond

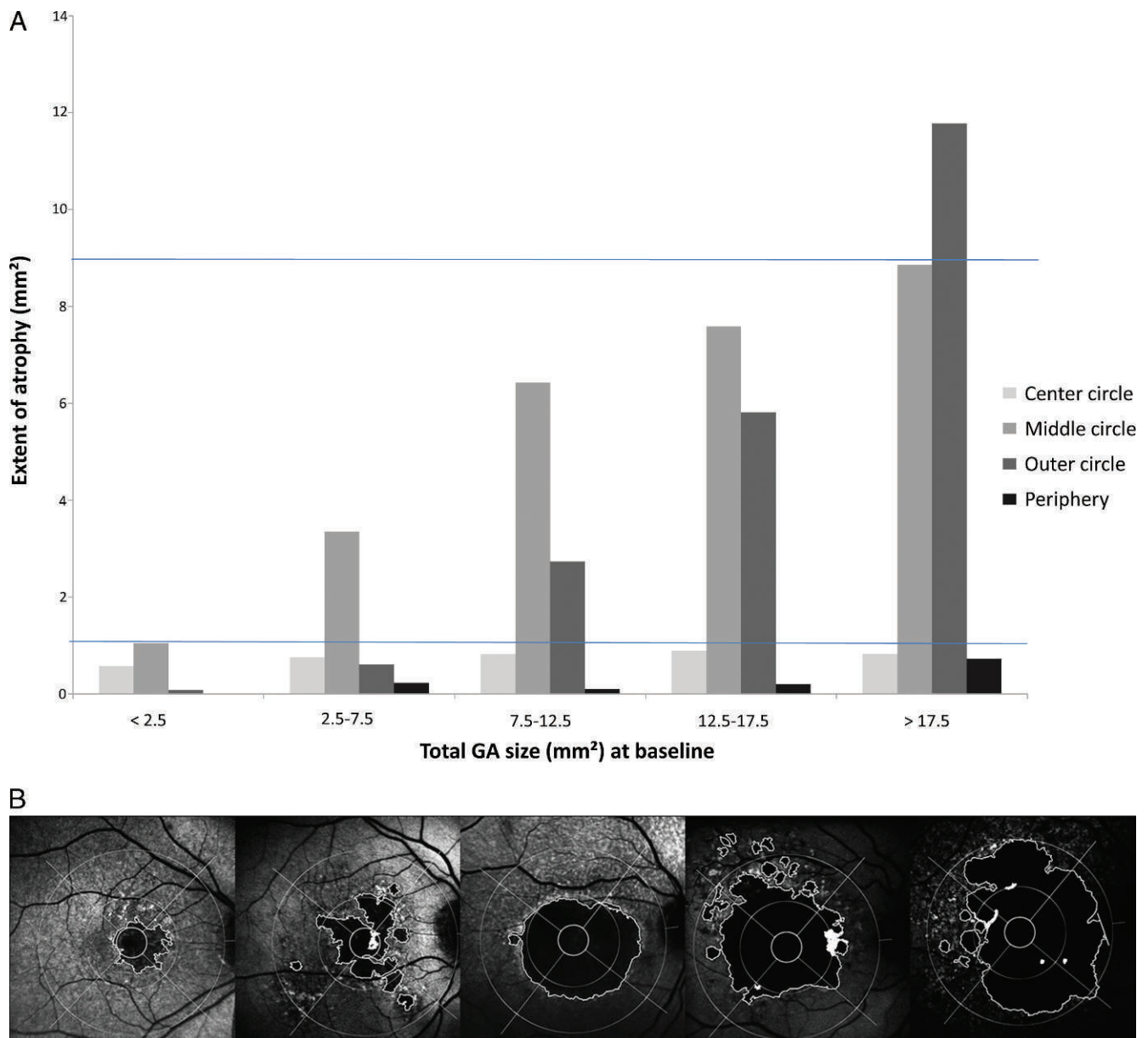


FIGURE 4. Topographic extent of atrophy in circles and periphery with respect to total size of atrophy. **(A)** Topography and total size of atrophy. The median size of each zone and of retinal areas beyond the grid (periphery) is shown for different ranges of total GA atrophy sizes. The columns for each cluster go from left to right as follows: center zone, inner zone, outer zone, and periphery (*lower horizontal line*: maximum size of the center zone; *upper horizontal line*: maximum size of the inner zone). **(B)** Representative examples for each of the five atrophy size ranges plotted in Figure 4A.

identically to the anatomical locations of the fovea, parafovea, and outer macular regions that may also vary among individuals. Similar caveats apply to the term foveal sparing; the exact clinical scenario whereby this term applies is unclear. Furthermore, it appears that the phenomenon of foveal sparing does not fully correspond to the maximum density of cones.⁹ Further studies with multimodal retinal imaging, including spectral-domain optical coherence tomography, are needed to specifically investigate the lesion growth toward the fovea in GA subjects.

In conclusion, this study demonstrates that the distribution and progression of GA patches depend on the localization within the macula and the total GA size. The parafoveal and foveal retina appear to be more susceptible to the occurrence and expansion of GA than the outer macula.

In addition, more extensive GA involvement of the retina superiorly in the outer macula may reflect a higher vulnerability at this anatomic site. This detailed analysis of distribution and directional GA spread is useful to understand the natural history of GA and will also be helpful to design future interventional clinical trials.

References

1. Gass JD. Drusen and disciform macular detachment and degeneration. *Arch Ophthalmol*. 1973;90:206-217.
2. Blair CJ. Geographic atrophy of the retinal pigment epithelium. A manifestation of senile macular degeneration. *Arch Ophthalmol*. 1975;93:19-25.

3. Schatz H, McDonald HR. Atrophic macular degeneration. Rate of spread of geographic atrophy and visual loss. *Ophthalmology*. 1989;96:1541-1551.
4. Sunness JS. The natural history of geographic atrophy, the advanced atrophic form of age-related macular degeneration. *Mol Vis*. 1999;5:25.
5. Sunness JS, Gonzalez-Baron J, Applegate CA, et al. Enlargement of atrophy and visual acuity loss in the geographic atrophy form of age-related macular degeneration. *Ophthalmology*. 1999;106:1768-1779.
6. Schmitz-Valckenberg S, Fleckenstein M, Helb HM, Charbel Issa P, Scholl HP, Holz FG. In-vivo imaging of foveal sparing in geographic atrophy secondary to age-related macular degeneration. *Invest Ophthalmol Vis Sci*. 2009;50:3915-3921.
7. Sunness JS, Bressler NM, Maguire MG. Scanning laser ophthalmoscopic analysis of the pattern of visual loss in age-related geographic atrophy of the macula. *Am J Ophthalmol*. 1995;119:143-151.
8. Chen C, Wu L, Wu D, et al. The local cone and rod system function in early age-related macular degeneration. *Doc Ophthalmol*. 2004;109:1-8.
9. Curcio CA. Photoreceptor topography in ageing and age-related maculopathy. *Eye*. 2001;15:376-383.
10. Curcio CA, Millican CL, Allen KA, Kalina RE. Aging of the human photoreceptor mosaic: evidence for selective vulnerability of rods in central retina. *Invest Ophthalmol Vis Sci*. 1993;34:3278-3296.
11. Jackson GR, Owsley C, Curcio CA. Photoreceptor degeneration and dysfunction in aging and age-related maculopathy. *Ageing Res Rev*. 2002;1:381-396.
12. Owsley C, Jackson GR, Cideciyan AV, et al. Psychophysical evidence for rod vulnerability in age-related macular degeneration. *Invest Ophthalmol Vis Sci*. 2000;41:267-273.
13. Scholl HP, Bellmann C, Dandekar SS, Bird AC, Fitzke FW. Photopic and scotopic fine matrix mapping of retinal areas of increased fundus autofluorescence in patients with age-related maculopathy. *Invest Ophthalmol Vis Sci*. 2004;45:574-583.
14. Chuang EL, Sharp DM, Fitzke FW, Kemp CM, Holden AL, Bird AC. Retinal dysfunction in central serous retinopathy. *Eye*. 1987;1(Pt 1):120-125.
15. Xu W, Grunwald JE, Metelitsina TI, et al. Association of risk factors for choroidal neovascularization in age-related macular degeneration with decreased foveolar choroidal circulation. *Am J Ophthalmol*. 2010;150:40-47.
16. Beatty S, Murray IJ, Henson DB, Carden D, Koh H, Boulton ME. Macular pigment and risk for age-related macular degeneration in subjects from a Northern European population. *Invest Ophthalmol Vis Sci*. 2001;42:439-446.
17. Delori FC, Dorey CK, Staurengi G, Arend O, Goger DG, Weiter JJ. In vivo fluorescence of the ocular fundus exhibits retinal pigment epithelium lipofuscin characteristics. *Invest Ophthalmol Vis Sci*. 1995;36:718-729.
18. von Ruckmann A, Fitzke FW, Bird AC. Distribution of fundus autofluorescence with a scanning laser ophthalmoscope. *Br J Ophthalmol*. 1995;79:407-412.
19. Deckert A, Schmitz-Valckenberg S, Jorzik J, Bindewald A, Holz FG, Mansmann U. Automated analysis of digital fundus autofluorescence images of geographic atrophy in advanced age-related macular degeneration using confocal scanning laser ophthalmoscopy (cSLO). *BMC Ophthalmol*. 2005;5:8.
20. Schmitz-Valckenberg S, Brinkmann CK, Alten F, et al. Semi-automated image processing method for identification and quantification of geographic atrophy in age-related macular degeneration. *Invest Ophthalmol Vis Sci*. 2011;52:7640-7646.
21. Holz FG, Bindewald-Wittich A, Fleckenstein M, Dreyhaupt J, Scholl H, Schmitz-Valckenberg S. Progression of geographic atrophy and impact of fundus autofluorescence patterns in age-related macular degeneration. *Am J Ophthalmol*. 2007;143:463-472.
22. Fleckenstein M, Adrion C, Schmitz-Valckenberg S, et al. Concordance of disease progression in bilateral geographic atrophy due to AMD. *Invest Ophthalmol Vis Sci*. 2009;51:637-642.
23. Sunness J, Margalit E, Srikurnaran D, et al. The long-term natural history of geographic atrophy from age-related macular degeneration. *Ophthalmology*. 2007;114:271-277.
24. Klein R, Meuer SM, Knudtson MD, Klein BE. The epidemiology of progression of pure geographic atrophy: the Beaver Dam Eye Study. *Am J Ophthalmol*. 2008;146:692-699.
25. Lindblad AS, Lloyd PC, Clemons TE, et al. Change in area of geographic atrophy in the Age-Related Eye Disease Study: AREDS report number 26. *Arch Ophthalmol*. 2009;127:1168-1174.
26. Bindewald A, Schmitz-Valckenberg S, Jorzik JJ, et al. Classification of abnormal fundus autofluorescence patterns in the junctional zone of geographic atrophy in patients with age related macular degeneration. *Br J Ophthalmol*. 2005;89:874-878.
27. Fleckenstein M, Schmitz-Valckenberg S, Adrion C, et al. Tracking progression with spectral-domain optical coherence tomography in geographic atrophy caused by age-related macular degeneration. *Invest Ophthalmol Vis Sci*. 2010;51:3846-3852.
28. Fleckenstein M, Schmitz-Valckenberg S, Adrion C, et al. Progression of age-related geographic atrophy: role of the fellow eye. *Invest Ophthalmol Vis Sci*. 2011;52:6552-6557.
29. Schmitz-Valckenberg S, Alten F, Steinberg JS, et al. Reticular drusen associated with geographic atrophy in age-related macular degeneration. *Invest Ophthalmol Vis Sci*. 2011;52:5009-5015.
30. Klein R, Meuer SM, Knudtson MD, Iyengar SK, Klein BE. The epidemiology of retinal reticular drusen. *Am J Ophthalmol*. 2008;145:317-326.
31. Rohrschneider K, Gluck R, Kruse FE, Volcker HE. [Location of the fovea at the fundus in relation to the optic nerve head]. *Ophthalmologie*. 1998;95:706-709.
32. Trauzettel-Klosinski S. Rehabilitation for visual disorders. *J Neuro-Ophthalmol*. 2010;30:73-84.

APPENDIX

The GAP Study was sponsored by Alcon Research Ltd. The following principal investigators were members of the GAP Study Group: H. J. Agostini (Freiburg, Germany); R. Anand (Dallas, TX); J. Arnold (Sydney); F. Bandello (Udine, Italy); D. S. Boyer (Beverly Hills, CA); D. M. Brown (Houston, TX); D. Callanan (Arlington, TX); U. Chakravarthy (Belfast, Ireland); G. Cowan (Forth Worth, TX); S. Downes (Oxford, United Kingdom); R. Guymer (Melbourne); L. S. Halperin (Ft. Lauderdale, FL); Y. G. He (Dallas, TX); J. S. Heier (Boston, MA); F. G. Holz (Bonn, Germany); A. Leys (Leuven, Belgium); A. Loewenstein (Tel Aviv); E. Midena (Padova, Italy); Patel (Abilene, TX); D. Pauleikhoff (Münster, Germany); A. Pollack (Rehovot); C. Prunte/M Georgopoulos (Vienna, Austria); S. R. Russell (Iowa City, IA); S. V. Sadda (Los Angeles, CA); L. Singerman (Cleveland, OH); J. A. Sahel/S Mohand-Said (Paris, France); G. Staurengi (Milano, Italy); M. P. Teske (Salt Lake City, UT); A. Tufail (London, United Kingdom); C. Von Strachwitz (Würzburg, Germany); J. A. Wells III (West Columbia, SC); P. Wiedemann (Leipzig, Germany); S. Wolf/U Wolf-Schnurrbusch (Bern, Switzerland). The following Alcon Research Ltd employees contributed to this study as Clinical Trial Managers: Alberta Davis, Petra Kozma-Wiebe, Miguel Martinez.